https://doi.org/10.3311/PPch.20522

Periodica Polytechnica Chemical Engineering, 67(1), pp. 83–93, 2023

Formaldehyde Adsorption and Sensing: A Density Functional Theory Study on Pd_4 Nanocluster Decorated CNT Structure

Numan Yuksel[1], Ahmet Kose[1], Mehmet Ferdi Fellah[1*]

[1] Department of Chemical Engineering, Faculty of Engineering and Natural Sciences, Bursa Technical University, Mimar Sinan Boulevard, 177 Eflak Street, 16310 Yıldırım, Bursa, Turkey
[*] Corresponding author, e-mail: mferdi.fellah@btu.edu.tr

Received: 24 May 2022, Accepted: 23 September 2022, Published online: 09 January 2023

Abstract

The sensing of formaldehyde, one of the volatile organic compounds used in chemical processes, is very important. In this study, the adsorption and sensing of formaldehyde molecule on Pd_4 nanocluster decorated carbon nanotube (Pd_4-CNT) was investigated by using DFT method. The WB97XD hybrid method was used in DFT calculations. The adsorption energy value was calculated as −8.1 kJ/mol. This low adsorption energy confirms the very short recovery time and the predominance of weak interactions. There was a decrease of approximately 20% in the HOMO-LUMO gap after the interaction. This result shows that the Pd_4-CNT can be used as a sensor at room temperature.

Keywords

DFT, Pd_4 nanocluster, formaldehyde, adsorption, sensor

1 Introduction

Formaldehyde (HCHO) is one of the remarkable volatile organic compounds with high chemical reactivity and thermal stability used as an intermediate in chemical processes [1]. HCHO, which is highly toxic and volatile gas, is one of the leading indoor air pollutants [2, 3]. In addition to its use in constructive and decorative materials, it is practiced in pharmacology, medicine and other chemical industries [1–4]. Exposure to formaldehyde over 100 ppb may cause serious disturbances in the respiratory system, eyes, nose, throat, nervous and endocrine systems [5]. For this reason, the detection of formaldehyde is part of today's research [5, 6]. Functional nanomaterials can improve the sensing sensitivity of sensors, shorten the sensing time, and further stabilize the physical and chemical properties of sensors, significantly improving the sensing performance of sensors [7–9]. Nanomaterials such as graphene [10], phosphorene [11], boron nitride nanocage [12], MoS_2 [13], and CNT [14], have been studied for detection and adsorption.

CNTs, with their excellent physical and mechanical properties, are used in the detection and adsorption of gases such as NO [15], NO_2 [16], CO [17], NH_3 [18], and HCHO [14]. However, it was found that the ability of pristine CNT to detect and adsorb gases is poor due to the Van der Waals interaction [19]. Hence, the studies have intensified to increase the ability to detect and sorption gases by modifying CNT with metals [20–22]. Zhou et al. [20] discovered that Al doped CNT had stronger adsorption/interaction than defected CNT and charge transfer from CNT to HCHO. In another formaldehyde adsorption study, the doping of Pd and Si atoms significantly improved the adsorption energy and electrical conductivity of CNT [23]. Especially, Pd atom strongly affects the chemical reactivity of support materials against gases, thanks to their high catalytic activity. So, the modification with Pd atom increases the interaction as well as improves the charge transfer process [24, 25]. In order to increase the catalytic effect of Pd atom, it is common to use nanoclusters in adsorption and catalytic studies of gases such as CO [26], CO_2 [27], NO [28], H_2 [29], and HCHO. Manna et al. [30] investigated HCHO adsorption in structures formed by functionalization of Pt, Au and Ag clusters on reduced graphene oxide (RGO). Additionally, in the research of the dehydrogenation mechanism of formaldehyde by DFT (density functional theory) method on Pt_4 cluster, the energy barrier value being less than 14 kcal/mol indicates the high catalytic feature of the Pt_4 cluster [31]. Considering the success of the use of noble

Cite this article as: Yuksel, N., Kose, A., Ferdi Fellah, M. "Formaldehyde Adsorption and Sensing: A Density Functional Theory Study on Pd_4 Nanocluster Decorated CNT Structure", Periodica Polytechnica Chemical Engineering, 67(1), pp. 83–93, 2023. https://doi.org/10.3311/PPch.20522

metals in literature, it is thought that the use of Pd_4 cluster as formaldehyde adsorbent will be successful. In addition, Cuong et al. [32] revealed that the most stable state of the Pt_4 nanocluster on CNT was the tetrahedral form used in this study. Another study in which the methane molecule was adsorbed was carried out by decorating Pt_4 and Pd_4 nanoclusters on CNT in tetrahedral form [33].

In this study, the adsorption and sensing properties of HCHO on Pd_4 tetrahedral nanocluster decorated CNT structure were investigated by DFT method.

2 Computational methods

The DFT method was used to perform the theoretical calculations in this study [34]. Gaussian09 software was used for all theoretical calculations [35]. The WB97XD (including dispersion) hybrid approach was used to account for the effects of exchange and correlation in DFT calculations [36]. The zigzag model (6,0) [35] single-wall CNT (SWCNT) structure (semi-metallic tube) which has been modeled as the cluster including 108 carbon atoms with 48 honeycomb rings has been utilized for DFT calculations in this research. Hydrogen (H) atoms are attached to the ends of the free carbon bonds of the nanotube. Pd_4 tetrahedral nanocluster was placed or decorated on the surface of the CNT structure. All atoms have been kept relaxed during all theoretical calculations utilized in this study. While the basis set of 6-31G(d,p) was utilized or the C, O and H atoms, the LANL2DZ basis set was used for Pd atoms. 6-31G(d,p) basis set for C, H and O atoms [37–39] and LANL2DZ basis set for metal atoms including Pd atom [38, 40, 41] are widely used in the literature. In addition, Yu et al. [39] proved that the results obtained by using 6-31G(d,p) basis set for the fenton reaction on the rGo-4-PP-Nc structure were in agreement with the experimental data. Equilibrium geometries (EGs) and energies were obtained as a result of DFT calculations. In present study, the correction for basis-set superposition error (BSSE) which have been utilized by the counterpoise method has not been taken into account in theoretical calculations utilized since this error generally gives small effects on these type DFT calculations. It has been reported in a theoretical study where DFT calculations have been utilized for carbon nanosheet, nanocone, nanotube and fullerene structures that the BSSE correction for the WB97XD hybrid method with 6-31G(d) basis set has been calculated as quite small (it has been approximately reported as 1 kcal/mol more negative) and the BSSE does not play important role [42, 43]. Furthermore, it has been stated in the literature that the BSSE has an effect in the range of 0.5–2 kcal/mol in DFT calculations and the BSSE is more important for MP2 theory levels [44, 45]. On the other hand, in present study, zero point energy (ZPE) corrections for energy values have been taken into account. These energy values were computed as follows:

$$E = E_{\text{electronic}} + \text{ZPE} + E_{\text{vibrational}} + E_{\text{rotational}} + E_{\text{translational}}, \quad (1)$$

$$H = E + RT. \quad (2)$$

Here E stands for the sum of electronic, zero-point, and thermal energies, H stands for the sum of electronic and thermal enthalpies, R is the global ideal gas constant, and T is temperature (298.15 K). Below equation was utilized to calculate the relative adsorption energy and adsorption enthalpy values for formaldehyde adsorption on Pd_4-CNT structure.

$$\Delta(E/H) = (E/H)_{\text{System}} - \left[(E/H)_{\text{Formaldehyde}} + (E/H)_{\text{Pd}_4\text{-CNT}}\right] \quad (3)$$

$(E/H)_{\text{System}}$, $(E/H)_{\text{Formaldehyde}}$ and $(E/H)_{\text{Pd}_4\text{-CNT}}$ were the thermal/enthalpy energy of adsorbate on the structure, formaldehyde molecule and the Pd_4-CNT structure, respectively. The convergence criteria applied in DFT calculations utilized in Gaussian software are 18×10^{-4} bohr for max displacement, 12×10^{-4} radian for gradients of root-mean-square (rms) displacement, 45×10^{-5} hartree/bohr for max force and 3×10^{-4} hartreee/radian for rms force during DFT computations utilized in this study. In addition, the SCF convergence criteria applied in DFT calculations utilized in Gaussian09 software [35] for rms change in the density matrix and maximum change in the density matrix were 1×10^{-8} and 1×10^{-6}, respectively. Moreover, no imaginary (negative) frequency was found in Hessian matrix for all DFT calculations. Multiwfn software has been used to obtain the Reduced Density Gradient (RDG) scatter graphs and isosurfaces of RDGs [46]. The Density of States (DOS) plots have been received by GaussSum software [47]. Additionally, NBO atomic charges were obtained by using Natural Bond Orbital (NBO) population analysis. The cartesian coordinates of all structures are given in Supplementary Material.

3 Results and discussion

HCHO molecule adsorption on CNT structure decorated with Pd_4 nanocluster was investigated using DFT calculations. First of all, in order to obtain the EG of the CNT structure, DFT calculations utilizing different Spin Multiplicity (SM) values were made by taking the total

charge as zero. The SM of the CNT structure was determined as singlet. After the CNT structure was optimized, four Pd atoms were attached on its surface in tetrahedral form by DFT calculation utilizing triplet SM. Then the Pd_4-CNT structure was also optimized. The optimized geometries of the pristine CNT and Pd_4-CNT structures were obtained, and they are shown in Fig. 1.

When the structural parameters in the optimized structure obtained by decorating the Pd_4 cluster on the CNT were examined, the Pd-Pd bond lengths in the Pd4 cluster were calculated to be 2.67 Å and 2.71 Å, and the Pd-C bond lengths were computed as 2.06, 2.13 and 2.13 Å. These structural characters are in agreement with the values found in the other Pd_4-CNT studies (2.65 Å [48], and 2.67 Å [49], for Pd-Pd bond lengths and 2.08 Å [48], for Pd-C bond length). The CNT structures used in these studies are (8,0) SWCNT and (5,5) SWCNT.

After the EG of the Pd_4-CNT structure was obtained, the HCHO molecule was attached to the Pd_4 surface of Pd_4-CNT structure. The optimized geometry of the HCHO/Pd_4-CNT system was obtained by performing DFT calculations and it is represented in Fig. 2. After HCHO adsorption, the adsorption energy (ΔE) was calculated as −8.1 kJ/mol and the adsorption enthalpy (ΔH) was computed to be −10.5 kJ/mol. This result shows that the HCHO molecule adsorption on the Pd_4-CNT structure is an exothermic process at ambient conditions. For the optimized HCHO molecule, the C=O and C-H bond lengths

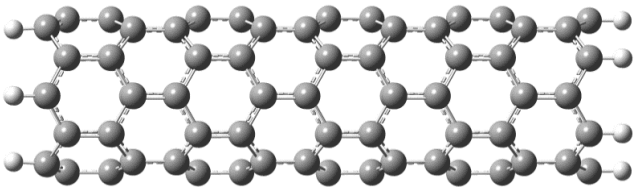

(a)

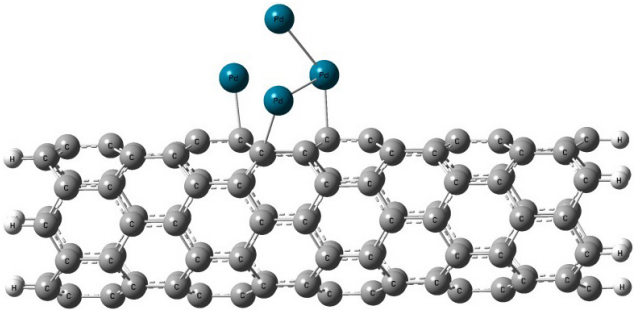

(b)

Fig. 1 The optimized geometries of (a) the pristine CNT structure and (b) Pd_4-CNT structure

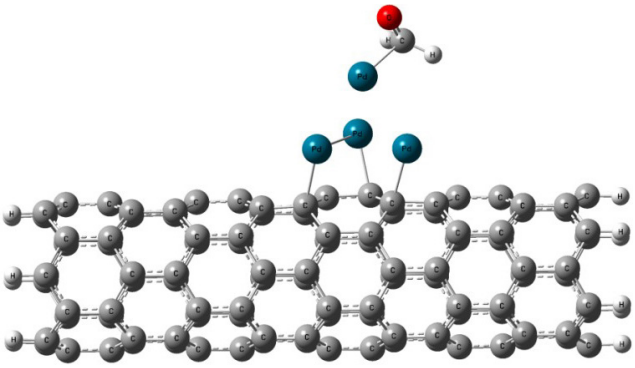

Fig. 2 The optimized geometry of HCHO/Pd_4-CNT system

are 1.20 and 1.11 Å. These values are in agreement with the results in the literature [50, 51]. After the adsorption process, the C=O and C-H bond lengths of HCHO molecule were found to be 1.26 and 1.10 Å, respectively. The elongation of the C=O bond after adsorption indicates the effect of the interaction. Additionally, the frequency values of ν_{CO}, ν_{CH2} (rock) and ν_{CH2} (wag) in the gas phase of HCHO were calculated as 1856, 1266 and 1198 cm^{-1}, respectively. The harmony of these frequencies with the experimentally found values is remarkable (ν_{CO}: 1746, ν_{CH2} (rock): 1249 and ν_{CH2} (wag): 1167 cm^{-1}) [52]. After adsorption of HCHO on Pd_4-CNT structure, the frequencies of ν_{CO}, ν_{CH2} (rock), ν_{CH2} (wag) were obtained as 1612, 1222 and 1051 cm^{-1}. These results support the interaction found between HCHO and Pd_4-CNT structure.

Carneiro and Cruz [53] found the adsorption energy of −55.2 kJ/mol for the HCHO adsorption on the Pd_4 tetrahedral cluster with the DFT method. The adsorption energy of HCHO on the Pd (111) surface was experimentally found in the range of −50.2 to −61.1 kJ/mol [54]. In addition, the energy value of HCHO on Pd doped CNT was reported as −112.9 kJ/mol [23]. Considering these results in the literature, it is seen that the Pd_4 nanocluster and the Pd doped CNT structure give better adsorption results with respect to sensor applications. The reason why the Pd_4 nanocluster on the CNT gives worse adsorption values than the single Pd atom on the CNT is due to the interaction of the Pd atoms with each other. Additionally, the reason why the Pd_4 nanocluster gives better results without the CNT structure is due to the interaction of the Pd_4 nanocluster and the CNT structure. B3LYP hybrid method was used in the study of Carneiro and Cruz [53]. To compare the methods and to see if the Pd_4 nanocluster really supports the CNT structure in the adsorption processes; HCHO adsorption was carried out on the Pd_4 nanocluster. The EG of HCHO on Pd_4 is shown in Fig. 3.

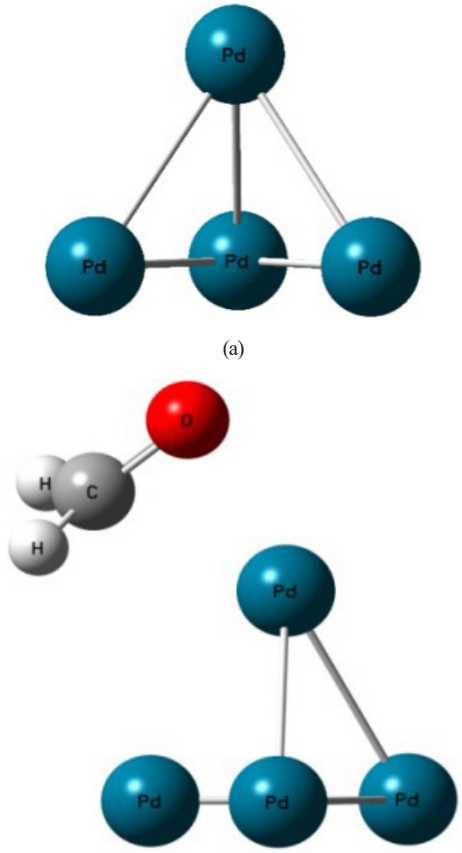

Fig. 3 The optimized geometries of (a) Pd_4 tetrahedral nanocluster and (b) HCHO adsorbed Pd_4 tetrahedral nanocluster

Because of the calculations, the ΔE value was calculated as −58.4 kJ/mol and the ΔH value as −60.8 kJ/mol. As mentioned before, the adsorption energy was reported as −55.2 kJ/mol on Pd_4 tetrahedral cluster in a theoretical study [53]. The reason for small difference between the results (−58.4 kJ/mol vs. −55.2 kJ/mol) was using different DFT methods (WB97XD vs B3LYP). As stated also before, the WB97XD method includes the dispersion effects. It takes into account the London dispersion forces resulting from instantaneous dipoles. Thus, the results were close to each other with the WB97XD hybrid method and the B3LYP hybrid method. Certainly, the WB97XD and B3LYP hybrid methods are different hybrid methods. It may be more accurate to compare the WB97XD and WB97X (without dispersion) and B3LYP and B3LYP-D3 (with dispersion) methods among themselves. But the difference between the B3LYP-D3 method and the WB97XD method is very small. Mounssef et al. [55] performed H_2 adsorption on two different clusters (6MR and 8MR clusters) of Cu-SSZ-13 zeolite and calculated their energy values. The adsorption energies on the 6MR cluster were calculated as −5.0 kcal/mol and −4.8 kcal/mol for the B3LYP-D3 and WB97XD methods, respectively. For the 8MR cluster, these values were determined as −15.0 kcal/mol and −14.8 kcal/mol [55]. According to these results, we can see the WB97XD and B3LYP-D3 hybrid methods as similar methods. Therefore, we can say that the difference between the WB97XD and B3LYP methods is the dispersion effects. In addition, the binding energy of the Pd_4 nanocluster to the CNT structure was calculated as −351.2 kJ/mol. This value shows that Pd_4-CNT is a very stable structure.

The effect of the Hartree-Fock (HF) percentages of the functionals is another important issue. Range Separated (RS) functionals vary the percentage of HF and DFT exchange for long-range and short-range interactions and are used in cases involving charge transfer excitation. WB97XD is an example of RS functionals. WB97XD is comprised of 22% HF exchange at the short range and 100% HF at the long range [56]. Global hybrid functionals use a constant percentage (20% for B3LYP) of exact HF exchange for both short-range and long-range. Since short-range interaction took place in this study, the HF percentages of the WB97XD and B3LYP functions are very close. Considering the energy results and the dispersion effects of the WB97XD method, we can say that the effect of these two functionals is the same when the HF percentages are the same.

In order to reveal the importance of the CNT structure, HCHO adsorption was also performed on the pristine CNT structure. The EG of HCHO on pristine CNT is shown in Fig. 4. According to the result of the adsorption study, the ΔE value was calculated as −12.4 kJ/mol and the ΔH value was computed to be −14.9 kJ/mol for HCHO on pristine CNT. These results show that the CNT structure and the Pd_4 nanocluster reduce each other's adsorption abilities, especially the CNT structure is more dominant in this negative effect.

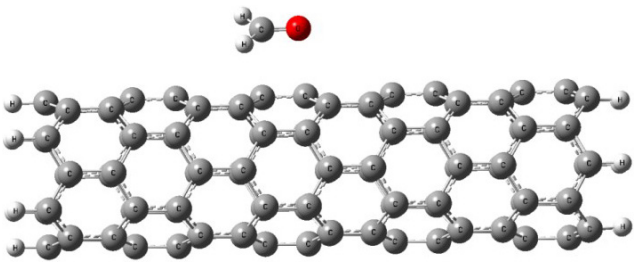

Fig. 4 The optimized geometry of HCHO adsorbed pristine CNT

HOMO (Highest Occupied Molecular Orbital) and LUMO (Lowest Unoccupied Molecular Orbital) energies were calculated and the change in HOMO-LUMO gap energy (E_g) values were analyzed to evaluate the electronic characteristics of Pd_4-CNT structure, Pd_4 nanocluster and CNT structure against HCHO molecule. Thus, the electronic sensor property of the Pd_4-CNT structure was determined and the effects of the Pd_4 nanocluster and the CNT structure were also revealed in this study. The HOMO and LUMO energies, E_g, ΔE_g and $\%\Delta E_g$ values of the Pd_4-CNT structure, Pd_4 nanocluster and pristine CNT structure before and after adsorption are tabulated in Table 1 for both α and β of the molecular orbitals (spin up and spin down, respectively).

The E_g value is calculated using Eq. (4):

$$E_g = \epsilon_{\text{LUMO}} - \epsilon_{\text{HOMO}}. \tag{4}$$

Changes in the E_g values of the constructs indicate approximately 20% reduction in the Pd_4-CNT structure. This magnitude reduction indicates that the Pd_4-CNT structure could be an electronic sensor against the HCHO molecule. On the other hand, the pristine CNT structure and Pd_4 nanocluster were virtually unchanged. Thus, it has been revealed that the Pd_4 nanocluster and the pristine CNT structure cannot be electronic sensors separately, and they come together and change their electronic properties. Because E_g has been shown many times to be a good indicator for determining the sensitivity of nanosensors [57]. There is also a relation between E_g and electrical conductivity (σ), which has also been mentioned [58, 59]:

$$\sigma = AT^{3/2} \exp\left[-E_g/(2\kappa T)\right]. \tag{5}$$

Table 1 Electronic properties of HCHO adsorbed Pd_4-CNT structure, Pd_4 nanocluster and pristine CNT structure (values are in units of kJ/mol)

Structure		ϵ_{HOMO}	ϵ_{LUMO}	E_g	ΔE_g	$\%\Delta E_g$
Pd_4	α MOs	−708.6	−35.6	673.0	–	–
	β MOs	−669.9	−115.8	554.0		
HCHO/Pd_4	α MOs	−729.4	−63.2	666.8	−6.8	−1.0
	β MOs	−711.8	−150.3	561.5	7.5	1.3
Pd_4-CNT	α MOs	−569.1	−194.1	374.9	–	–
	β MOs	−584.3	−192.3	391.9		
HCHO/ Pd_4-CNT	α MOs	−577.5	−212.2	365.2	−9.6	−2.5
	β MOs	−527.1	−210.7	316.3	−75.6	−19.2
Pristine CNT	$\alpha + \beta$ MOs	−432.7	−238.8	194.3	–	–
HCHO/ Pristine CNT	$\alpha + \beta$ MOs	−432.8	−239.9	192.9	−1.4	−0.7

Here κ is the Boltzmann's constant, A (electrons/$m^3K^{3/2}$) is a constant value and T is temperature. Equation (5) points to that the reducing in E_g increases the population of conduction electrons exponentially. Therefore, because of the chemical which is existed in the environment, it causes an increase in electrical conductivity. The sensor response factor (R) is defined in Eq. (6) to predict the magnitude of the electrical change [60]:

$$R = \sigma_2/\sigma_1 = \exp\left[-\left(\left(E_{g2} - E_{g1}\right)/(2\kappa T)\right)\right] = \exp\left(-\Delta E_g/2\kappa T\right). \tag{6}$$

Here σ_1 and σ_2 are the electrical conductivity signals of the Pd_4-CNT structure and HCHO adsorbed Pd_4-CNT structure, respectively. It was determined that the R values calculated for α and β molecular orbitals and the ΔE_g values were proportional. Accordingly, the R values are 6.93 and 3.79×10^6 for α and β, respectively. According to this result, it can be said that the Pd_4-CNT structure has a high sensitivity to the HCHO molecule. In addition, NBO atomic charge distributions were calculated in this study. After HCHO on the Pd_4-CNT structure, the NBO total charge of the HCHO molecule was calculated as −0.200e. While the NBO total charge of the Pd_4 nanocluster in the Pd_4-CNT structure was +0.399e before adsorption, it was calculated as +0.501e after HCHO adsorption. These results indicate that the charge transfer is occurred from the HCHO molecule to the Pd_4 nanocluster on the surface of the CNT structure.

The HOMO-LUMO representations of Pd_4-CNT structure and HCHO adsorbed Pd_4-CNT structure have been presented in Figs. 5 and 6. As shown in Figs. 5 and 6, the most significant interaction between the Pd_4-CNT structure and the HCHO molecule after adsorption occurs in the β MOs spin. It is also the spin at which E_g decreases the most. In addition, the presence and changes of HOMOs and LUMOs around the Pd_4 nanocluster before and after adsorption reveals the importance of the Pd_4 nanocluster for the interaction with HCHO molecule.

Chemical hardness (η), chemical potential (μ), electronegativity (χ) and electrophilicity (ω) values of the Pd_4-CNT structure were calculated and listed in Table 2. After adsorption, the chemical hardness of the Pd_4-CNT structure slightly decreased. Thus, it has become a softer structure. The increase in the chemical potential of the structure shows that there is a slight increase in the chemical reactivity, and the decrease in the electronegativity at the same rate indicates that the stability is slightly

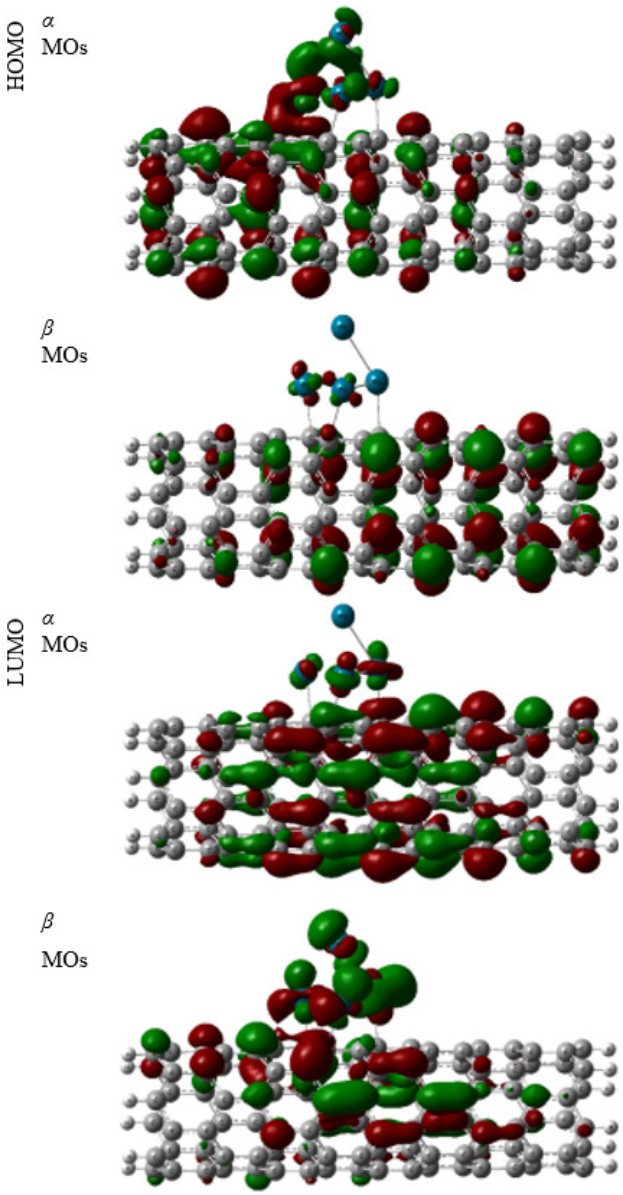

Fig. 5 HOMO/LUMO distributions for the Pd_4-CNT structure

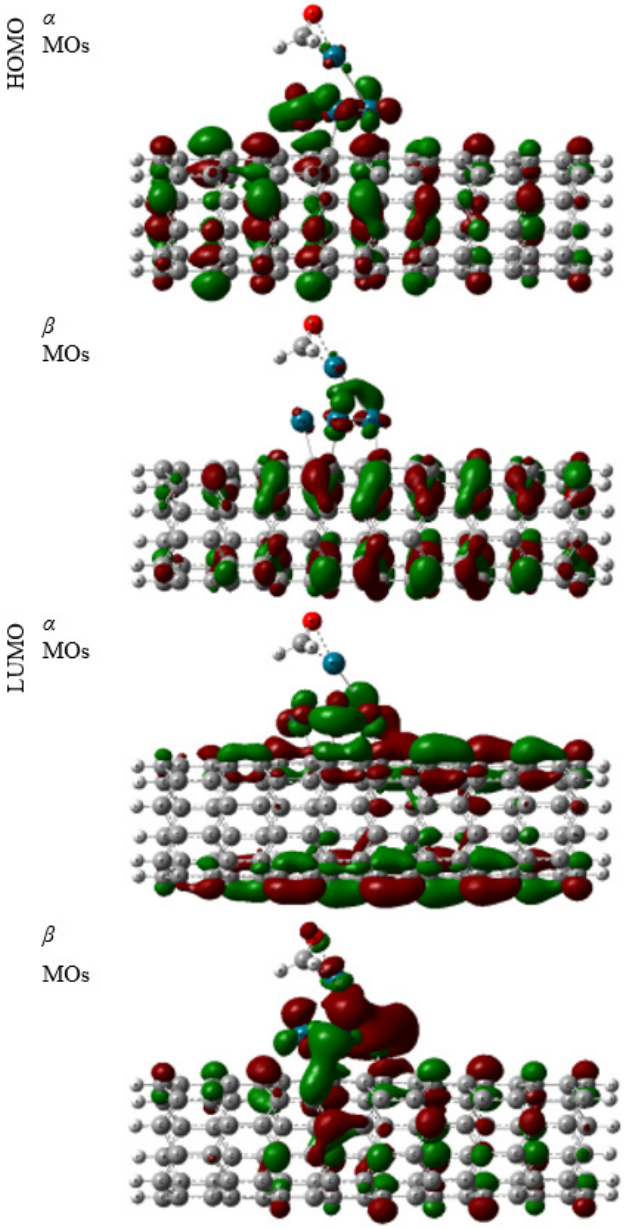

Fig. 6 HOMO/LUMO distributions for the HCHO/Pd_4-CNT system

decreased. The electrophilicity of the structure, which refers to the sensor property, is in a significant increase.

The density of states (DOS) of Pd_4-CNT structure and HCHO molecule adsorbed Pd_4-CNT structure have been presented in Fig. 7. The DOS plots show the changes in the E_g for both α MOs and β MOs. Accordingly, the decrease in E_g, especially the decrease in β MOs, is very clearly seen. This result implies that the electrical conductivity increases in the Pd_4-CNT structure after HCHO adsorption. The sensor capabilities of CNT structures in humidity mediums have been investigated in previous research. CNT structures functionalized with $MoSe_2$ were found to be sensitive to dimethylformamide and ammonia in humidity environment studies [61, 62]. In addition, Liu et al. [63] experimentally observed that the carbon nanotube-based sensor is capable of successfully detecting formaldehyde in relative humidity environments. These results show that the Pd-doped CNT structure will also give good results under humidity conditions.

Table 2 The η, μ, χ and ω values for the optimized Pd_4-CNT before and after HCHO adsorption (values are in units of kJ/mol)

Structure		η	μ	χ	ω
Pd_4-CNT	α MOs	187.47	−381.66	381.66	388.50
	β MOs	195.95	−388.35	388.35	384.81
HCHO/Pd_4-CNT	α MOs	182.64	−394.86	394.86	462.83
	β MOs	158.16	−368.93	368.93	430.29

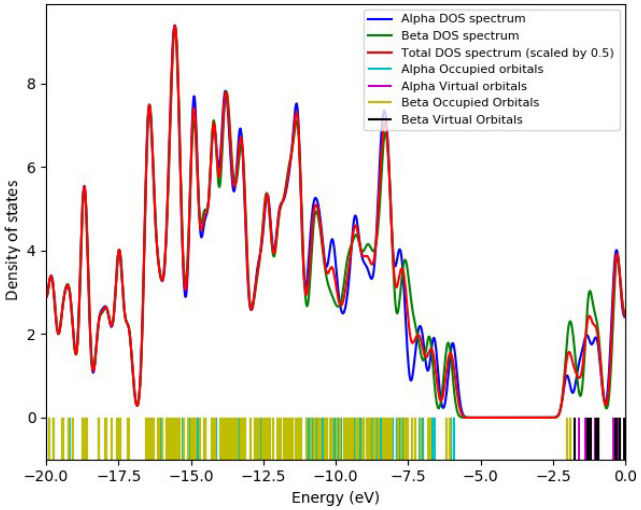

(a)

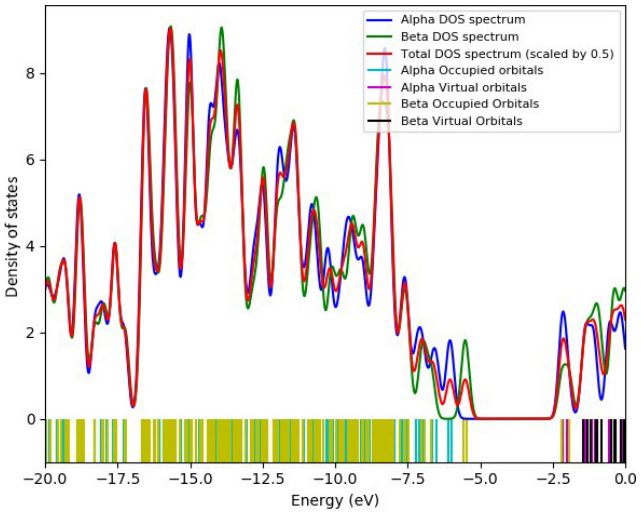

(b)

Fig. 7 The DOS plots for the (a) Pd_4-CNT structure and (b) HCHO/Pd_4-CNT system

The analysis for reduced density gradient (RDG) has been proposed by Johnson et al. [64], which allows obtaining the type of interactions occur between two species. RDG analysis has been used to examine the many non-covalent interactions remaining in the molecules, the reduced gradient of the density as a function of the electron density multiplied by the sign of the second eigenvalue of the matrix of Hessian matrix. The greatest eigenvalue in the Hessian matrix is known to be λ_2. It describes the variations of the density in the vicinity of the critical point. It could be used to differentiate between the different kinds of noncovalent interactions. Fig. 8 presents RDG scatter graph and isosurface of RDG for HCHO adsorbed on Pd_4-CNT structure. Strong attractive interactions, weak interactions and repulsive interactions have been represented in blue color, in green color and in red color, respectively. Based on the

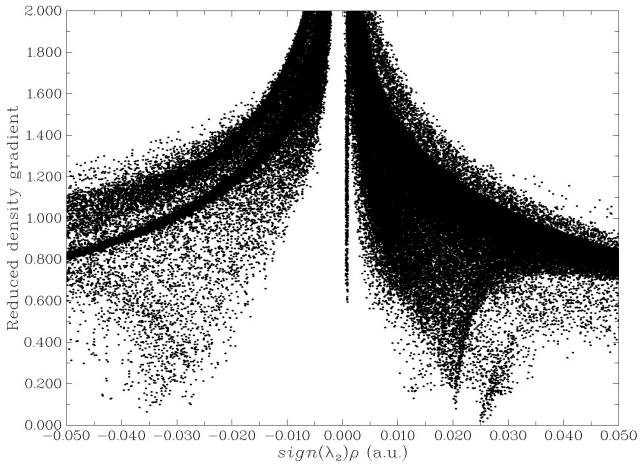

(a)

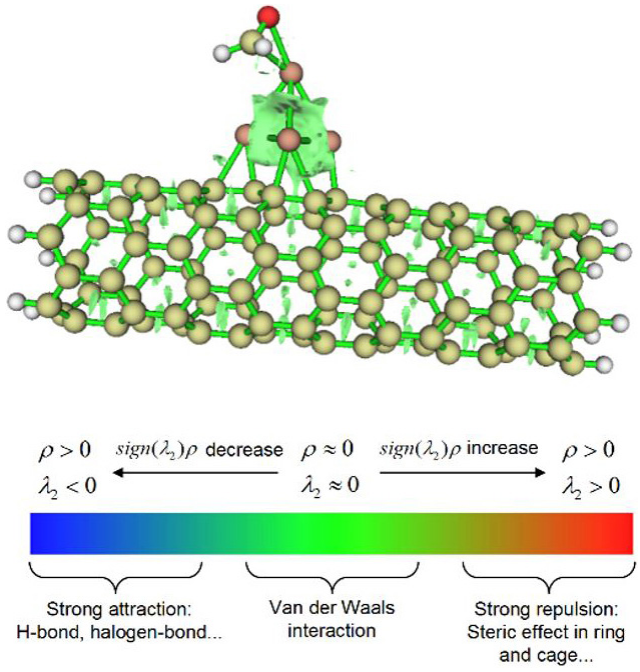

(b)

Fig. 8 RDG analysis (a) RDG scatter graph for optimized geometry of HCHO/Pd_4-CNT system and (b) isosurface of RDG for optimized geometry of HCHO/Pd_4-CNT system

RDG analysis, VdW interactions are shown with near-zero values marked in green. The RDG scatter plot and isosurface map tells us that the interaction between the HCHO molecule and the Pd_4-CNT structure is typically governed by weak VdW-type interactions.

Likewise, the electrostatic potential (ESP) distribution map for the Pd_4-CNT structure and the HCHO/Pd_4-CNT system is presented in Fig. 9. The positive and negative areas of the Van der Waals surface are defined in blue and red colors on the ESP maps [64, 65]. The ESP decreases by different colors in order to red < yellow < blue. According to Fig. 9, it is seen that red colors are formed on the side of

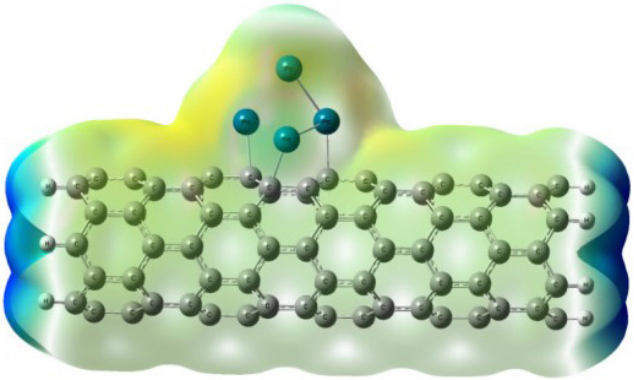

(a)

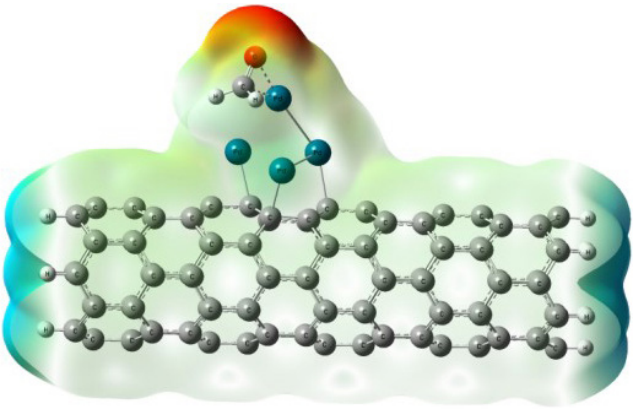

(b)

Fig. 9 ESP distribution maps for (a) Pd_4-CNT structure and (b) HCHO/Pd_4-CNT system

the HCHO molecule after adsorption. Therefore, it shows that the ESP decreases and negative fields are formed on the side of the HCHO. This result refers to the negative total charge of the HCHO in charge transfer.

There is a relationship between the adsorption energy and desorption of the adsorbate. The greater the adsorption energy, the longer the traditional transition theory predicts a recovery time. Equation (7) can be used to explain this situation:

$$\tau = (\nu_0)^{-1} \exp(-E_{ad}/\kappa T) \cdot \quad (7)$$

Here the recovery time is τ, adsorption energy is E_{ad}, adsorption temperature is T (298.15 K), κ is the constant of Boltzmann (~8.368×10^{-3} kJ/mol) and the ν_0 is attempt frequency (~10^{12} s^{-1}) [16]. More negative E_{ad} values increase the recovery times exponentially, according to Eq. (7). The recovery time was calculated as 10^{-10} s for Pd_4-CNT structure. This is an expected result due to the low E_{ad}.

4 Conclusions

In this study, HCHO on Pd_4-CNT structure was investigated by DFT method. The results show that the Pd_4-CNT structure with negative adsorption energy can be used as an adsorbent. In addition, it was revealed that a Pd_4 nanocluster was decorated into the CNT structure and lower adsorption energy was found in the study. This result shows that Pd atoms interact with each other in the Pd_4 nanocluster. According to the sensor properties obtained by DFT calculations, it shows ~20% reduction in E_g of the Pd_4-CNT structure, so that it can be used as a sensor against HCHO molecule at room conditions. In addition, it was determined that Van der Waals interactions were effective between the Pd_4-CNT structure and the HCHO molecule. The effects of Pd_4 nanocluster and CNT structure on this powerful sensor property were also investigated. In the studies performed with the Pd_4 nanocluster and the pristine CNT structure, no sensor properties were observed. Thus, it was observed that the Pd_4 nanocluster and the CNT structure came together and changed their electronic properties positively and supported each other. It has been consequently mentioned that carbon structures decorated with nanoclusters will give better sensor properties in detecting formaldehyde-like chemicals.

Acknowledgement

The numerical calculations reported in this paper were in part completed at ULAKBIM/TUBITAK, High Performance and Grid Computing Center (the resources of TRUBA).

References

[1] Teng, B.-T., Jiang, S.-Y., Yang, Z.-X., Luo, M.-F., Lan, Y.-Z. "A density functional theory study of formaldehyde adsorption and oxidation on CeO_2(1 1 1) surface", Surface Science, 604(1), pp. 68–78, 2010. https://doi.org/10.1016/j.susc.2009.10.024

[2] Akyavaşoğlu, Ö., Fellah, M. F. "A DFT Study of Si Doped Graphene: Adsorption of Formaldehyde and Acetaldehyde", Turkish Computational and Theoretical Chemistry, 4(1), pp. 39–48, 2020. https://doi.org/10.33435/tcandtc.691754

[3] Chen, Z., He, X., Ge, J., Fan, G., Zhang, L., Parvez, A. M., Wang, G. "Controllable fabrication of nanofibrillated cellulose supported HKUST-1 hierarchically porous membranes for highly efficient removal of formaldehyde in air", Industrial Crops and Products, 186, 115269, 2022. https://doi.org/10.1016/j.indcrop.2022.115269

[4] Gazzari, S., Cortés-Arriagada, D. "Uptake of formaldehyde onto doped phosphorene nanosheets: A cluster DFT study of single and co-adsorption states", Journal of Alloys and Compounds, 831, 154885, 2020. https://doi.org/10.1016/j.jallcom.2020.154885

[5] Liu, H., Zhao, M., Lei, Y., Pan, C., Xiao, W. "Formaldehyde on TiO_2 anatase (1 0 1): A DFT study", Computational Materials Science, 51(1), pp. 389–395, 2012. https://doi.org/10.1016/j.commatsci.2011.07.048

[6] Liu, L., Zhao, J. "Formaldehyde adsorption and decomposition on rutile (110): A first-principles study", Surface Science, 652, pp. 156–162, 2016. https://doi.org/10.1016/j.susc.2015.12.036

[7] He, J., Xu, P., Zhou, R., Li, H., Zu, H., Zhang, J., Qin, Y., Liu, X., Wang, F. "Combustion Synthesized Electrospun InZnO Nanowires for Ultraviolet Photodetectors", Advanced Electronic Materials, 8(4), 2100997, 2022. https://doi.org/10.1002/aelm.202100997

[8] Li, T., Shang, D., Gao, S., Wang, B., Kong, H., Yang, G., Shu, W., Xu, P., Wei, G. "Two-Dimensional Material-Based Electrochemical Sensors/Biosensors for Food Safety and Biomolecular Detection", Biosensors, 12(5), 314, 2022. https://doi.org/10.3390/bios12050314

[9] Wang, Y., Wu, X., Liu, J., Zhai, Z., Yang, Z., Xia, J., Deng, S., Qu, X., Zhang, H., Wu, D., Wang, J., Fu, C., Zhang, Q. "Mo-modified band structure and enhanced photocatalytic properties of tin oxide quantum dots for visible-light driven degradation of antibiotic contaminants", Journal of Environmental Chemical Engineering, 10(1), 107091, 2022. https://doi.org/10.1016/j.jece.2021.107091

[10] Zhou, Q., Yuan, L., Yang, X., Fu, Z., Tang, Y., Wang, C., Zhang, H. "DFT study of formaldehyde adsorption on vacancy defected graphene doped with B, N, and S", Chemical Physics, 440, pp. 80–86, 2014. https://doi.org/10.1016/j.chemphys.2014.06.016

[11] Ghadiri, M., Ghashghaee, M., Ghambarian, M. "Defective phosphorene for highly efficient formaldehyde detection: Periodic density functional calculations", Physics Letters A, 384(31), 126792, 2020. https://doi.org/10.1016/j.physleta.2020.126792

[12] Rostami, Z., Pashangpour, M., Moradi, R. "DFT study on the chemical sensing properties of $B_{24}N_{24}$ nanocage toward formaldehyde", Journal of Molecular Graphics and Modelling, 72, pp. 129–135, 2017. https://doi.org/10.1016/j.jmgm.2016.12.013

[13] Deng, X., Liang, X., Ng, S.-P., Wu, C.-M. L. "Adsorption of formaldehyde on transition metal doped monolayer MoS_2: A DFT study", Applied Surface Science, 484, pp. 1244–1252, 2019. https://doi.org/10.1016/j.apsusc.2019.04.175

[14] Dwivedi, N., Shukla R. K. "Theoretical study of pure/doped (nitrogen and boron) carbon nanotubes for chemical sensing of formaldehyde", SN Applied Sciences, 2(2), 262, 2020. https://doi.org/10.1007/s42452-020-2055-2

[15] Jia, X., An, L., Chen, T. "Adsorption of nitrogen oxides on Al-doped carbon nanotubes: The first principles study", Adsorption, 26(4), pp. 587–595, 2020. https://doi.org/10.1007/s10450-020-00218-3

[16] Peng, S., Cho, K., Qi, P., Dai, H. "Ab initio study of CNT NO_2 gas sensor", Chemical Physics Letters, 387(4–6), pp. 271–276, 2004. https://doi.org/10.1016/j.cplett.2004.02.026

[17] Santucci, S., Picozzi, S., Di Gregorio, F., Lozzi, L., Cantalini, C., Valentini, L., Kenny, J. M., Delley, B. "NO_2 and CO gas adsorption on carbon nanotubes: Experiment and theory", The Journal of Chemical Physics, 119(20), pp. 10904–10910, 2003. https://doi.org/10.1063/1.1619948

[18] Chang, H., Lee, J. D., Lee, S. M., Lee, Y. H. "Adsorption of NH_3 and NO_2 molecules on carbon nanotubes", Applied Physics Letters, 79(23), pp. 3863–3865, 2001. https://doi.org/10.1063/1.1424069

[19] Yoosefian, M., Raissi, H., Mola, A. "The hybrid of Pd and SWCNT (Pd loaded on SWCNT) as an efficient sensor for the formaldehyde molecule detection: A DFT study", Sensors and Actuators B: Chemical, 212, pp. 55–62, 2015. https://doi.org/10.1016/j.snb.2015.02.004

[20] Zhou, Q., Wang, C., Fu, Z., Zhang, H., Tang, Y. "Adsorption of formaldehyde molecule on Al-doped vacancy-defected single-walled carbon nanotubes: A theoretical study", Computational Material Science, 82, pp. 337–344, 2014. https://doi.org/10.1016/j.commatsci.2013.09.046

[21] Gebhardt, J., Bosch, S., Hof, F., Hauke, F., Hirsch, A., Görling, A. "Selective reduction of SWCNTs – concepts and insights", Journal of Material Chemistry C, 5(16), pp. 3937–3947, 2017. https://doi.org/10.1039/C5TC01407G

[22] Billing, B. K., Agnihotri, P. K., Singh, N. "Fabrication of branched nanostructures for CNT@Ag nano-hybrids: application in CO_2 gas detection", Journal of Material Chemistry C, 5(17), pp. 4226–4235, 2017. https://doi.org/10.1039/C7TC00984D

[23] Zhou, X., Zhao, C., Chen, C., Chen, J., Li, Y. "DFT study on adsorption of formaldehyde on pure, Pd-doped, Si-doped single-walled carbon nanotube", Applied Surface Science, 525, 146595, 2020. https://doi.org/10.1016/j.apsusc.2020.146595

[24] Yoosefian, M. "Powerful greenhouse gas nitrous oxide adsorption onto intrinsic and Pd doped Single walled carbon nanotube", Applied Surface Science, 392, pp. 225–230, 2017. https://doi.org/10.1016/j.apsusc.2016.09.051

[25] Shi, J., Quan, W., Chen, X., Chen, X., Zhang, Y., Lv, W., Yang, J., Zeng, M., Wei, H., Hu, N., Su, Y., Zhou, Z., Yang, Z. "Noble metal (Ag, Au, Pd and Pt) doped TaS_2 monolayer for gas sensing: a first-principles investigation", Physical Chemistry Chemical Physics, 23(34), pp. 18359–18368, 2021. https://doi.org/10.1039/D1CP02011K

[26] Kalita, B., Deka, R. C. "Adsorption of CO on oxygen preadsorbed neutral and charged gas phase Pd_4 clusters: A density functional study", Journal of Computational Chemistry, 31(13), pp. 2476–2482, 2010. https://doi.org/10.1002/jcc.21541

[27] Batista, K. E. A., Ocampo-Restrepo, V. K., Soares, M. D., Quiles, M. G., Piotrowski, M. J., Da Silva, J. L. F. "*Ab Initio* Investigation of CO_2 Adsorption on 13-Atom 4d Clusters", Journal of Chemical Information and Modeling, 60(2), pp. 537–545, 2020. https://doi.org/10.1021/acs.jcim.9b00792

[28] Lacaze-Dufaure, C., Roques, J., Mijoule, C., Sicilia, E., Russo, N., Alexiev, V., Mineva, T. "A DFT study of the NO adsorption on Pd_n (n = 1–4) clusters", Journal of Molecular Catalysis A: Chemical, 341(1–2), pp. 28–34, 2011. https://doi.org/10.1016/j.molcata.2011.03.020

[29] Sen, D., Thapa, R., Chattopadhyay, K. K. "Small Pd cluster adsorbed double vacancy defect graphene sheet for hydrogen storage: A first-principles study", International Journal of Hydrogen Energy, 38(7), pp. 3041–3049, 2013. https://doi.org/10.1016/j.ijhydene.2012.12.113

[30] Manna, B., Chakrabarti, I., Guha, P. K. "First Principles Study of Noble Metal (Single Atom and Cluster) Decorated Reduced Graphene Oxide for Efficient Formaldehyde Adsorption", IEEE Sensors Journal, 21(3), pp. 2544–2551, 2020. https://doi.org/10.1109/JSEN.2020.3022077

[31] Phan, T. T., Dao, L. T. T., Giang, L. P. T., Nguyen, M. T., Nguyen, H. M. T. "Mechanistic insights into the dehydrogenation of formaldehyde, formic acid and methanol using the Pt_4 cluster as a promising catalyst", Journal of Molecular Graphics and Modelling, 111, 108096, 2022. https://doi.org/10.1016/j.jmgm.2021.108096

[32] Cuong, N. T., Sugiyama, A., Fujiwara, A., Mitani, T., Chi, D. H. "Density functional study of Pt_4 clusters adsorbed on a carbon nanotube support", Physical Review B, 79(23), 235417, 2009. https://doi.org/10.1103/PhysRevB.79.235417

[33] Russell, J., Zapol, P., Král, P., Curtiss, L. A. "Methane bond activation by Pt and Pd subnanometer clusters supported on graphene and carbon nanotubes", Chemical Physics Letters, 536, pp. 9–13, 2012. https://doi.org/10.1016/j.cplett.2012.03.080

[34] Kohn, W., Sham, L. J. "Self-Consistent Equations Including Exchange and Correlation Effects", Physical Review, 140(4A), pp. A1133–A1138, 1965. https://doi.org/10.1103/PhysRev.140.A1133

[35] Frisch, M., Trucks, G., Schlegel, H., Scuseria, G., Robb, M., Cheeseman, J., Scalmani, G., Barone, V., Mennucci, B., Petersson, G. Ochter-ski, J. W., Martin, R. L., Morokuma, K., Zakrzewski, V. G., Voth, G. A., Salvador, P., Dannenberg, J. J., Dapprich, S., Daniels, A. D., Farkas, O., Foresman, J. B., Ortiz, J. V., Cioslowski, J., Fox, D. J. "Gaussian 09, Revision D.01", Gaussian Inc., Wallingford, CT, USA, 2013.

[36] Chai, J.-D., Head-Gordon, M. "Systematic optimization of long-range corrected hybrid density functionals", The Journal of Chemical Physics, 128(8), 084106, 2008. https://doi.org/10.1063/1.2834918

[37] Fellah, M. F. "CO and NO Adsorptions on Different Iron Sites of Fe-ZSM-5 Clusters: A Density Functional Theory Study", The Journal of Physical Chemistry C, 115(5), pp. 1940–1951, 2011. https://doi.org/10.1021/jp107534n

[38] Zhang, X., Gong, X. "DFT, QTAIM, and NBO investigations of the ability of the Fe or Ni doped CNT to absorb and sense CO and NO", Journal of Molecular Modelling, 21(9), 225, 2015. https://doi.org/10.1007/s00894-015-2778-y

[39] Yu, G., Lyu, L., Zhang, F., Yan, D., Cao, W., Hu, C. "Theoretical and experimental evidence for rGO-4-PP Nc as a metal-free Fenton-like catalyst by tuning the electron distribution", RSC Advances, 8(6), pp. 3312–3320, 2018. https://doi.org/10.1039/C7RA12573A

[40] Buasaeng, P., Rakrai, W., Wanno, B., Tabtimsai, C. "DFT investigation of NH_3, PH_3, and AsH_3 adsorptions on Sc-, Ti-, V-, and Cr-doped single-walled carbon nanotubes", Applied Surface Science, 400, pp. 506–514, 2017. https://doi.org/10.1016/j.apsusc.2016.12.215

[41] Yoosefian, M., Barzgari, Z., Yoosefian, J. "Ab initio study of Pd-decorated single-walled carbon nanotube with C-vacancy as CO sensor", Structural Chemistry, 25(1), pp. 9–19, 2014. https://doi.org/10.1007/s11224-013-0220-6

[42] Kobko, N., Dannenberg, J. J. "Effect of Basis Set Superposition Error (BSSE) upon ab Initio Calculations of Organic transition states", Journal of Physical Chemistry A, 105(10), pp. 1944–1950, 2001. https://doi.org/10.1021/jp001970b

[43] Vessally, E., Alkorta, I., Ahmadi, S., Mohammadi, R., Hosseinian, A. "A DFT study on nanocones, nanotubes (4,0), nanosheets and fullerene C_{60} as anodes in Mg-ion batteries", RSC Advances, 9(2), pp. 853–862, 2019. https://doi.org/10.1039/C8RA06031B

[44] Volk, D. E., Thiviyanathan, V., Somasunderam, A., Gorenstein, D. G. "*Ab initio* base-pairing energies of an oxidized thymine product, 5-formyluracil, with standard DNA bases at the BSSE-free DFT and MP2 theory levels", Organic & Biomolecular Chemistry, 5(10), pp. 1554–1558, 2007. https://doi.org/10.1039/B702755A

[45] Shields, A. E., van Mourik T. "Comparison of ab Initio and DFT Electronic Structure Methods for Peptides Containing an Aromatic Ring: Effect of Dispersion and BSSE", The Journal of Physical Chemistry A, 111(50), pp. 13272–13277, 2007. https://doi.org/10.1021/jp076496p

[46] Lu, T., Chen, F. "Multiwfn: A multifunctional wavefunction analyzer", Journal of Computational Chemistry, 33(5), pp. 580–592, 2012. https://doi.org/10.1002/jcc.22885

[47] Mulliken, R. S. "Electronic Population Analysis on LCAO–MO Molecular Wave Functions. I", The Journal of Chemical Physics, 23(10), pp. 1833–1840, 1955. https://doi.org/10.1063/1.1740588

[48] Cui, H., Zhang, X., Zhang, J., Tang, J. "Adsorption behaviour of SF6 decomposed species onto Pd_4-decorated single-walled CNT: a DFT study", Molecular Physics, 116(13), pp. 1749–1755, 2018. https://doi.org/10.1080/00268976.2018.1451930

[49] Cao, C., He, Y., Cheng, H.-P. "First-principles simulations of dissociated and molecular H_2 adsorption on Pd_4-cluster-functionalized carbon nanotubes", Physical Review B, 77(4), 045412, 2008. https://doi.org/10.1103/PhysRevB.77.045412

[50] Chen, X., Xu, L., Liu, L.-L., Zhao, L.-S., Chen, C.-P., Zhang, Y., Wang, X.-C. "Adsorption of formaldehyde molecule on the pristine and transition metal doped graphene: First-principles study", Applied Surface Science, 396, pp. 1020–1025, 2017. https://doi.org/10.1016/j.apsusc.2016.11.080

[51] Ma, D., Ju, W., Li, T., Yang, G., He, C., Ma, B., Tang, Y., Lu, Z., Yang, Z. "Formaldehyde molecule adsorption on the doped monolayer MoS_2: A first-principles study", Applied Surface Science, 371, pp. 180–188, 2016. https://doi.org/10.1016/j.apsusc.2016.02.230

[52] Busca, G., Lamotte, J., Lavalley, J. C., Lorenzelli, V. "FT-IR study of the adsorption and transformation of formaldehyde on oxide surfaces", Journal of the American Chemical Society, 109(17), pp. 5197–5202, 1987. https://doi.org/10.1021/ja00251a025

[53] Carneiro, J. W. D. M., Cruz, M. T. D. M. "Density Functional Theory Study of the Adsorption of Formaldehyde on Pd4 and on Pd_4/γ-Al_2O_3 Clusters", The Journal of Physical Chemistry A, 112(38), pp. 8929–8937, 2008. https://doi.org/10.1021/jp801591z

[54] Davis, J. L., Barteau, M. A. "Polymerization and decarbonylation reactions of aldehydes on the Pd(111) surface", Journal of the American Chemical Society, 111(5), pp. 1782–1792, 1989. https://doi.org/10.1021/ja00187a035

[55] Mounssef Jr., B., de Alcântara Morais, S. F., de Lima Batista, A. P., de Lima, L. W., Braga, A. A. C. "DFT study of H_2 adsorption at a Cu-SSZ-13 zeolite: a cluster approach", Physical Chemistry Chemical Physics, 23(16), pp. 9980–9990, 2021. https://doi.org/10.1039/d1cp00422k

[56] Halsey-Moore, C., Jena, P., McLeskey Jr., J. T. "Tuning range-separated DFT functionals for modeling the peak absorption of MEH-PPV polymer in various solvents", Computational and Theoretical Chemistry, 1162, 112506, 2019. https://doi.org/10.1016/j.comptc.2019.112506

[57] Perry, R. H., Green, D. W., Maloney, J. O. "Perry's Chemical Engineers' Handbook", McGraw-Hill, 1997. ISBN 0-07-049841-5

[58] Fellah, M. F. "Pt doped (8,0) single wall carbon nanotube as hydrogen sensor: A density functional theory study", International Journal of Hydrogen Energy, 44(49), pp. 27010–27021, 2019. https://doi.org/10.1016/j.ijhydene.2019.08.169

[59] Ahmadi, A., Hadipour, N. L., Kamfiroozi, M., Bagheri, Z. "Theoretical study of aluminum nitride nanotubes for chemical sensing of formaldehyde", Sensors and Actuators B: Chemical, 161(1) pp. 1025–1029, 2012. https://doi.org/10.1016/j.snb.2011.12.001

[60] Li, L., Zhao, J. "Defected boron nitride nanosheet as an electronic sensor for 4-aminophenol: A density functional theory study", Journal of Molecular Liquids, 306, 112926, 2020. https://doi.org/10.1016/j.molliq.2020.112926

[61] Singh, S., Deb, J., Kumar, S., Sarkar, U., Sharma, S. "Selective *N*,*N*-Dimethylformamide Vapor Sensing Using $MoSe_2$/Multiwalled Carbon Nanotube Composites at Room Temperature", ACS Applied Nano Materials, 5(3), pp. 3913–3924, 2022. https://doi.org/10.1021/acsanm.1c04505

[62] Singh, S., Deb, J., Sarkar, D., Sharma, S. "$MoSe_2$/multiwalled carbon nanotube composite for ammonia sensing in natural humid environment", Journal of Hazardous Materials, 435, 128821, 2022. https://doi.org/10.1016/j.jhazmat.2022.128821

[63] Liu, C., Hu, J., Wu, G., Cao, J., Zhang, Z., Zhang, Y. "Carbon Nanotube-Based Field-Effect Transistor-Type Sensor with a Sensing Gate for Ppb-Level Formaldehyde Detection", ACS Applied Material Interfaces, 13(47), pp. 56309–56319, 2021. https://doi.org/10.1021/acsami.1c17044

[64] Johnson, E. R., Keinan, S., Mori-Sánchez, P., Contreas-García, J., Cohen, A. J., Yang, W. "Revealing Noncovalent Interactions", Journal of the American Chemical Society, 132(18), pp. 6498–6506, 2010. https://doi.org/10.1021/ja100936w

[65] Sjoberg, P., Politzer, P. "Use of the electrostatic potential at the molecular surface to interpret and predict nucleophilic processes", The Journal of Physical Chemistry, 94(10), pp. 3959–3961, 1990. https://doi.org/10.1021/j100373a017